Research Article

Journal of Molecular Recognition

Received: 16 September 2013, Revised: 16 December 2013, Accepted: 16 December 2013, Published online in Wiley Online Library

(wileyonlinelibrary.com) DOI: 10.1002/jmr.2352

Direct and indirect interactions in the recognition between a cross-neutralizing antibody and the four serotypes of dengue virus

Olesia Lisova[a,b], Laurent Belkadi[a,b,c] and Hugues Bedouelle[a,b]*

Dengue fever is the most important vector-borne viral disease. Four serotypes of dengue virus, DENV1 to DENV4, coexist. Secondary infection by a different serotype is a risk factor for severe dengue. Monoclonal antibody mAb4E11 neutralizes the four serotypes of DENV with varying efficacies by recognizing an epitope located within domain-III (ED3) of the viral envelope (E) protein. To better understand the cross-reactivities between mAb4E11 and the four serotypes of DENV, we constructed mutations in both Fab4E11 fragment and ED3, and we searched for indirect interactions in the crystal structures of the four complexes. According to the serotype, 7 to 12 interactions are mediated by one water molecule, 1 to 10 by two water molecules, and several of these interactions are conserved between serotypes. Most interfacial water molecules make hydrogen bonds with both antibody and antigen. Some residues or atomic groups are engaged in both direct and water-mediated interactions. The doubly-indirect interactions are more numerous in the complex of lowest affinity. The third complementarity determining region of the light chain (L-CDR3) of mAb4E11 does not contact ED3. The structures and double-mutant thermodynamic cycles showed that the effects of (hyper)-mutations in L-CDR3 on affinity were caused by conformational changes and indirect interactions with ED3 through other CDRs. Exchanges of residues between ED3 serotypes showed that their effects on affinity were context dependent. Thus, conformational changes, structural context, and indirect interactions should be included when studying cross-reactivity between antibodies and different serotypes of viral antigens for a better design of diagnostics, vaccine, and therapeutic tools against DENV and other *Flaviviruses*.

Additional supporting information may be found in the online version of this article at the publisher's website.

Keywords: cross-reactivity; dengue virus; flavivirus; indirect interactions; neutralizing antibody; serotype; structure; water molecules

INTRODUCTION

Dengue is a mosquito-borne infection of the tropics and subtropics. Some 2.5 billion people are at risk, and 50–100 million are infected annually. Most infections are either asymptomatic or result in dengue fever, a relatively mild illness. However, a life-threatening form, severe dengue, develops in 1%–5% of infections (Simmons *et al*., 2012).

Dengue viruses have been classified into four serotypes, differing in overall amino acid sequence by ≥30% (Chen and Vasilakis, 2011). Infection by the dengue virus (DENV) raises lifelong immunity against the infecting serotype but only transient protection against the other serotypes (Sabin, 1952). Subsequent infections by viruses from different DENV serotypes are associated with a greater risk for severe dengue (Sangkawibha *et al*., 1984). The preferential reactivation of the memory B and T cells that correspond to a primary infection and an antibody-dependent enhancement of infection constitute triggering mechanisms of severe dengue during a secondary infection by a different viral serotype (Halstead *et al*., 2010; Midgley *et al*., 2011).

The dengue viruses are enveloped RNA viruses. The structure of the whole virus has been solved by electron cryomicroscopy (Zhang *et al*., 2013b; Zhang *et al*., 2013a). Ninety dimers of the envelope (E) protein cover the surface of the virus. The structure of the E protein has been solved by X-ray crystallography, either in a free state or in complex with an antibody (Modis *et al*., 2003; Zhang *et al*., 2004; Modis *et al*., 2005; Cockburn *et al*., 2012b). Each E protein monomer comprises three ectodomains, ED1 to ED3, and a transmembrane segment. ED2 includes the dimerization interface, glycosylation sites, and the peptide of fusion with the cellular membrane. ED3 is continuous and comprises residues 296–400 of the E protein (DENV1 numbering). Its fold is compact, immunoglobulin-like, and stabilized by a disulfide bond. The structures of recombinant ED3 domains have been

* *Correspondence to: Hugues Bedouelle, CNRS, URA3012, rue du Dr. Roux, F-75015 Paris, France.*
E-mail: hugues.bedouelle@pasteur.fr

a *O. Lisova, L. Belkadi, H. Bedouelle*
Institut Pasteur, Unit of Molecular Prevention and Therapy of Human Diseases, Department of Infection and Epidemiology, rue du Dr. Roux, F-75015 Paris, France

b *O. Lisova, L. Belkadi, H. Bedouelle*
CNRS, URA3012, rue du Dr. Roux, F-75015 Paris, France

c *L. Belkadi*
Present address: CNRS, UMR7138, Quai Saint-Bernard, F-75005 Paris, France

solved by X-ray crystallography or NMR methods, either in a free state or in complex with an antibody (Volk *et al.*, 2007; Huang *et al.*, 2008; Lok *et al.*, 2008; Simonelli *et al.*, 2010; Austin *et al.*, 2012; Cockburn *et al.*, 2012a; Midgley *et al.*, 2012; Elahi *et al.*, 2013; Simonelli *et al.*, 2013). The structure of the isolated ED3 domain is close to its structure in the E protein.

The ED3 domain has important functions and applications. It participates in the interaction between the virus and primary or secondary cell receptors, including heparan sulfates and ribosomal protein SA (Chen *et al.*, 1996; Thullier *et al.*, 2001; Pattnaik *et al.*, 2007; Huerta *et al.*, 2008; Watterson *et al.*, 2012; Zidane *et al.*, 2013b). Consistently, recombinant ED3 domains from DENV1 and DENV2 inhibit infectivity of the cognate virus (Hung *et al.*, 2004; Jaiswal *et al.*, 2004; Chin *et al.*, 2007). Mutations in the ED3 domain of DENV2 (ED3.DENV2) affect its cell tropism, replication, and virulence (Pryor *et al.*, 2001; Roehrig *et al.*, 2013). ED3 contains epitopes for neutralizing IgM and IgG antibodies, both in mice and in humans (Lok *et al.*, 2001; Lisova *et al.*, 2007; Gromowski *et al.*, 2008; Matsui *et al.*, 2009; Beltramello *et al.*, 2010; de Alwis *et al.*, 2011; Smith *et al.*, 2013).

The ED3 domains are used as antigens in immunoassays to detect infections by DENV (Simmons *et al.*, 1998b; Holbrook *et al.*, 2004; Batra *et al.*, 2011; Zidane *et al.*, 2013c). They are also used as immunogens in vaccine candidates against DENV (Schmitz *et al.*, 2011). The four serotypes of ED3 elicit neutralizing and protective antibodies in mice (Simmons *et al.*, 1998a; Chen *et al.*, 2007; Zhang *et al.*, 2007; Babu *et al.*, 2008; Etemad *et al.*, 2008; Guzman *et al.*, 2010). ED3.DENV2 and a consensus ED3 domain elicit neutralizing antibodies and partial protection in nonhuman primates (Guzman *et al.*, 2010; Chen *et al.*, 2013). Genes coding for ED3 domains have been inserted in the genome of infective nonpathogenic viruses and the recombinant viruses found to elicit neutralizing antibodies in mice (Brandler *et al.*, 2007; Khanam *et al.*, 2009; Brandler *et al.*, 2010).

Previously, we have reported that the mouse monoclonal antibody mAb4E11 neutralizes the four serotypes of DENV with variable efficacies and that its Fab fragment recognizes the four serotypes of the ED3 domain with dissociation constants (K_D) ranging from 0.082 nM for ED3.DENV1 to 4100 nM for ED3.DENV4. We have solved the structures of the complexes between the variable fragment (single-chain Fv [scFv]) of mAb4E11 and the ED3 domains from the four DENV serotypes by X-ray crystallography, at resolutions between 1.60 and 2.10 Å (Cockburn *et al.*, 2012a). The overall structures of the four complexes are very similar. scFv4E11 contacts ED3 through all its complementarity determining regions (CDR), except L-CDR3. We have mapped the energetic epitope of Fab4E11 in ED3.DENV1 and the paratope of ED3.DENV1 in Fab4E11 by mutagenesis. Mutations of L-CDR3 residues into alanine strongly increase the value of K_D for the interaction between Fab4E11 and ED3.DENV1 (Bedouelle *et al.*, 2006; Lisova *et al.*, 2007).

Here, given the importance of the ED3 domain for the life cycle of the virus and for applications and the importance of serotype cross-reactivities for the clinical outcome of dengue, we analyzed the roles of several direct and indirect interactions in the differential recognition between mAb4E11 and the four serotypes of ED3. First, we analyzed the contribution of water to this recognition. Water is known to play an important role in mediating the interactions between proteins (Janin, 1999; Barillari *et al.*, 2007; Ahmed *et al.*, 2011). Second, we analyzed the contacts between L-CDR3 and the other CDR loops of scFv4E11 and used double mutant thermodynamic cycles to understand how mutations, and in particular somatic hypermutations in L-CDR3, affect the affinity between Fab4E11 and ED3. Third, to understand the origin of the affinity differences between Fab4E11 and the four serotypes of ED3, we changed each of the residues of ED3.DENV1 that belong to its energetic epitope into the corresponding residues of the three other ED3 serotypes by mutagenesis of ED3.DENV1. We also introduced progressively the epitope of mAb4E11 from ED3.DENV1 into ED3.DENV4.

The results provided informations of general interest on the recognitions between mAb4E11 and the ED3 domains, in particular the following: (i) on the role of the interfacial water molecules; (ii) on the mechanisms of indirect interactions, mediated by CDR loops; and (iii) on the impact of the structural context in the contribution of epitope residues to the energy of interaction. These informations should be useful to engineer the ED3 domain or neutralizing antibodies and thus obtain efficient diagnostic, vaccine, or therapeutic tools against dengue.

MATERIALS AND METHODS

Viral and plasmid strains

The viral strains of DENV (Zidane *et al.*, 2013a), plasmids pPE1, pLB5 (Bedouelle *et al.*, 2006), pLB11, and pLB14 (Brandler *et al.*, 2007; Lisova *et al.*, 2007), have been described. pPE1 codes for a hybrid Fab4E11-H6 between the Fab fragment of mAb4E11 and a hexahistidine tag. pLB5 codes for a hybrid MalE-ED3.DENV1-H6 between the maltose binding protein MalE from *Escherichia coli*, the ED3 domain from DENV1, and a histidine tag. pLB11 and pLB14 code for hybrids ED3.DENV1-H6 and ED3.DENV4-H6 between the ED3 domains from DENV1 and DENV4, respectively, and a histidine tag.

DNA and protein methods

The mutagenesis of plasmids, the production of the encoded proteins in the periplasmic space of *E. coli*, and their purification to homogeneity by affinity chromatography from periplasmic extracts were performed as described (Bedouelle *et al.*, 2006; Lisova *et al.*, 2007). The correct folding of the wild type and mutant ED3-H6 domains and, in particular, the correct formation of their unique disulfide bond were checked by recording their fluorescence spectra and performing an Ellman's test, as described (Lisova *et al.*, 2007; Zidane *et al.*, 2013a). The determination of the dissociation constants (K_D) at equilibrium and 25 °C in solution by competition ELISA was performed exactly as described (Bedouelle *et al.*, 2006; Lisova *et al.*, 2007).

Sequence and structure analyses

We used Kabat's scheme for the numbering of the amino-acid sequence of immunoglobulins, as implemented in A.C.R. Martin's website (www.bioinf.org.uk/abs/abnum/), and Chothia's scheme for the definition of the CDR loops (Al-Lazikani *et al.*, 1997). The murine germline gene segments from which mAb4E11 and mAb1A1D-2 derive have already been reported (Bedouelle *et al.*, 2006; Cockburn *et al.*, 2012a). The atomic coordinates of the protein complexes were retrieved from the Worldwide protein data bank (www.wwpdb.org). The accession numbers were the following: 1FLR for the complex between Fab4-4-20 and fluorescein; 2R69 for the complex between Fab1A1D-2 and ED3.DENV2; 3UZQ, 3UZV, 3UZE, and 3UYP for the complexes between scFv4E11 and the ED3 domains from DENV1, DENV2,

DENV3, and DENV4, respectively. The structures of these last four complexes are known at resolutions of 1.60, 2.10, 2.04, and 2.00 Å, respectively. The structures were analyzed with the WHAT IF software package (Vriend, 1990). The accessible surface areas were computed with the ACCESS program and its VACACC subroutine; the contacts and hydrogen bonds between molecules with the ANACON program and CONTAC subroutine; the φ and ψ diedral angles with the CHIANG program and its SHOCHI sub-routine; and the indirect interactions through water molecules with the WATER program and its DBLWAT, NALWAT and WATNAA subroutines. The WHAT IF subroutines calculate the energy of hydrogen bonds on a scale from 0.00 to 1.00. The structures were drawn with RasMol version 2.7.3 (www.rasmol.org).

RESULTS

Indirect interactions through water molecules

The ED3 domains and the scFv fragment of mAb4E11 make indirect interactions, mediated by a single water molecule, in addition to numerous direct interactions (Supplementary Table S1). There are 12 water molecules involved in such indirect interactions for the ED3.DENV1 domain, 7 for DENV2, 7 for DENV3 and 12 for DENV4. Two of these indirect interactions are common to all four serotypes and involve the main chain oxygen atoms of residues Val/Ile/Met312 and Lys/Thr388 in ED3. Other indirect interactions are common to a smaller number of serotypes, for example, ED3.DENV1 and ED3.DENV4 have six indirect interactions in common. Most bridging water molecules are hydrogen bonded to both scFv4E11 and ED3.

Other indirect interactions are mediated by two-bridging water molecules (Supplementary Table S2). There are 5 couples of water molecules involved in such doubly indirect interactions for the ED3.DENV1 domain, 1 for DENV2, 2 for DENV3 and 10 for DENV4. Some of the doubly indirect interactions are conserved between several serotypes of ED3, that is, those involving Gln/Lys323, Glu327, or Ser/Asn390.

Many of the ED3 residues that make singly indirect interactions are already involved in direct interactions with scFv4E11 although not necessarily through the same atoms (Supplementary Table S3). Likewise, many of the ED3 residues that make doubly indirect interactions are already involved in direct or singly indirect interactions with scFv4E11. This is particularly the case for ED3.DENV4 for which 6 out of 10 doubly indirect interactions are made through Lys310 and Glu311, which are conserved and make the same direct interactions with scFv4E11 for all serotypes (Supplementary Table S2).

Indirect interactions between L-CDR3 of scFv4E11 and ED3.DENV1

The H-CDR3 loop of mAb4E11 includes the following seven residues: H-Gly95-Trp-Glu-Gly-Phe99-Ala101-Tyr102. The changes of Phe99, Ala101, or Tyr102 into Ala or Gly do not affect the free energy of interaction between Fab4E11 and ED3.DENV1 significantly, with $|\Delta\Delta G| \leq 0.4$ kcal mol^{-1}. In contrast, the changes of the four other residues into Ala strongly affect the interaction energy, with $\Delta\Delta G \geq 3.2$ kcal mol^{-1}. In particular, the changes H-E97A and H-W96A result in $\Delta\Delta G$ values of 5.7 ± 0.3 and >5.8 kcal mol^{-1}, respectively. The L-CDR3 loop of mAb4E11 includes nine residues: L-Gln89-Arg-Ser-Asn-Glu-Val-Pro-Trp-Thr97. The changes of Glu93, Val94, or Thr97 into Ala do not affect the interaction energy between Fab4E11 and ED3.DENV1 significantly, with $|\Delta\Delta G| \leq 0.3$ kcal mol^{-1}. In contrast, the changes of the six other residues into Ala affect the interaction energy, with $\Delta\Delta G \geq 1.1$ kcal mol^{-1} (Bedouelle *et al*., 2006). Nevertheless, the L-CDR3 loop of scFv4E11 does not make any direct interaction with ED3.DENV1 in the crystal structure of their complex (Cockburn *et al*., 2012a). We observed that several side chains of L-CDR3 make contacts with other CDR loops that, in turn, form direct contacts with ED3. We therefore analyzed whether mutations in L-CDR3 could affect the interaction with ED3 indirectly, through conformational changes.

The conformation of L-CDR3 depends on several intraloop H-bonds (Figure 1A). Mutations L-Q89A ($\Delta\Delta G = 1.6 \pm 0.1$ kcal mol^{-1}) and L-R90A ($\Delta\Delta G = 1.1 \pm 0.1$ kcal mol^{-1}) remove some of these intraloop H-bonds, and may therefore change the conformation of L-CDR3 and its interactions with the other CDR loops (Figure 1B). The study of these changes will be reported later in subsequent paragraphs.

Residues L-Ser91 in L-CDR3 and H-Trp96 in H-CDR3 make two H-bonds, between the Oγ-H group of L-Ser91 and the main-chain O atom of H-Trp96 and between the main-chain O atom of L-Ser91 and the Nε1-H group of H-Trp96. Thus, L-Ser91 constrains the side chain of H-Trp96 on the COOH side of this residue (Figure 1B). H-Trp96 makes extensive interactions with the antigen (Figure 1C) (Cockburn *et al*., 2012a). Thus, mutation L-S91A ($\Delta\Delta G = 2.9 \pm 0.1$ kcal mol^{-1}) could perturb the conformation of residue H-Trp96 and its interaction with the antigen.

Residue L-Asn92 in L-CDR3 makes two H-bonds with residues of L-CDR1, one between the Nδ2-H$_2$ group of L-Asn92 and the main-chain O atom of L-Asn27a and the other one between the main-chain O atom of L-Asn92 and the Nη1-H group of L-Arg27d. L-Asn92 is a structure determining residue of L-CDR1 in mAb4E11 (Bedouelle *et al*., 2006). L-Arg27d makes contacts with the antigen, in particular, with the Oε2 atom of Glu311 (Figure 1C) (Cockburn *et al*., 2012a). Thus, mutation L-N92A ($\Delta\Delta G = 1.1 \pm 0.1$ kcal mol^{-1}) could destabilize the conformation of L-CDR1 and affect the interaction of Fab4E11 with its antigen through L-Arg27d.

Residue L-Pro95 has a *cis* conformation (Figures 1A and 1B). Therefore, mutation L-P95A ($\Delta\Delta G = 2.9 \pm 0.1$ kcal mol^{-1}) changes the conformation of residue L-95 to a *trans* conformation, and consequently the conformation of L-CDR3, its interactions with the neighboring CDRs, and indirectly the interactions between Fab4E11 and its antigen.

The aromatic ring of residue L-Trp96 makes several contacts with the aromatic ring of H-Trp96 (Figure 1B). Therefore, mutation L-W96A ($\Delta\Delta G = 3.9 \pm 0.2$ kcal mol^{-1}) could strongly affect the interaction between Fab4E11 and its antigen through H-Trp96. Thus, the structural data on the complex between scFv4E11 and ED3.DENV1 are consistent with indirect effects of mutations in L-CDR3 on the interaction between scFv4E11 and its antigen.

Hypermutation L-Q90R

mAb4E11 contains 12 somatic hypermutations, six in the H-chain variable domain V_H, and six in the L-chain variable domain V_L, excluding the residues resulting from V-(D)-J recombinations. Five of these hypermutations are in CDR loops and the remaining seven, in framework regions (Supplementary Table S4) (Bedouelle *et al*., 2006). Because mAb4E11 was raised against DENV1, we analyzed the positions of the hypermutated residues

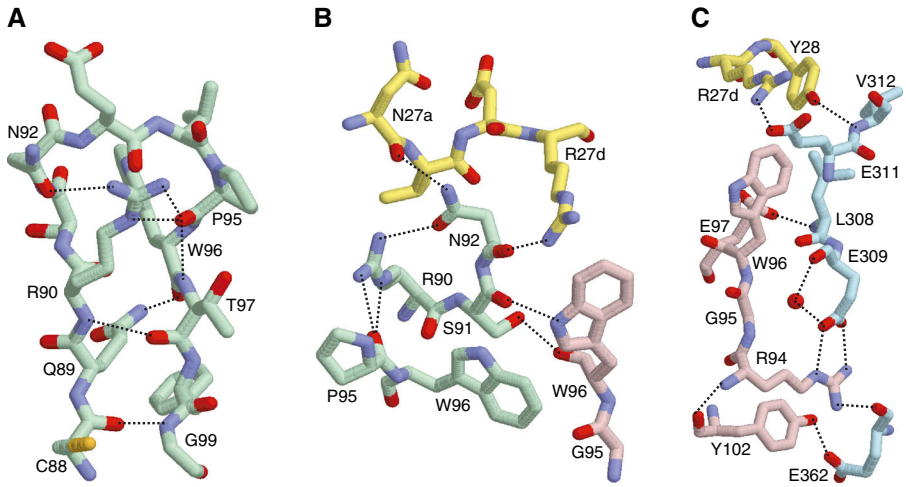

Figure 1. Direct and indirect interactions between scFv4E11 and ED3.DENV1 in their complex. L-CDR1 is coloured in yellow, L-CDR3 in green, H-CDR3 in pink, and ED3.DENV1 in light-blue. (A) Main interactions within L-CDR3. (B) Interactions of L-CDR3 with L-CDR1 and H-CDR3. (C) Interactions of L-CDR1 and H-CDR3 with ED3.DENV1. The potential H-bonds are represented by dashed lines. Lys325 was not represented in panel (C) for clarity. The figure was drawn from the PDB file 3UZQ.

in the structure of the complex between scFv4E11 and ED3.DENV1. None of the hypermutated residues interacts directly with the antigen except L-Arg27d, which belongs to L-CDR1 and whose side chain makes interactions with Glu311 in ED3.DENV1 (Figure 1C).

In particular, residue L-Arg90 results from the somatic hypermutation L-Q90R. We observed that residue L-Arg90 of scFv4E11 does not make any direct or indirect contact with the antigen in the structure of the complex with ED3.DENV1, and yet, mutation L-R90A decreases the energy of interaction between Fab4E11 and ED3.DENV1 by 1.1 ± 0.1 kcal mol^{-1} (Bedouelle *et al*., 2006; Cockburn *et al*., 2012a). To further analyze the role of this hypermutation, we reverted it by constructing mutation L-R90Q in Fab4E11, at the genetic level. We found that L-R90Q decreased the energy of interaction between Fab4E11 and ED3.DENV1 by 2.1 ± 0.2 kcal mol^{-1} (Table 1). Therefore, hypermutation L-Q90R stabilized the interaction between Fab4E11 and ED3.DENV1 by -2.1 kcal mol^{-1}. These results led us to assume that both mutations L-Q90R and L-R90A modify the conformation of Fab4E11 and, as a result, its interaction with the antigen.

Table 1. Equilibrium constants and associated free energies for the dissociation between MalE-ED3.DENV1-H6 and wild type or mutant Fab4E11-H6

Mutation	K_D (nM)	ΔG (kcal mol^{-1})	$\Delta\Delta G$ (kcal mol^{-1})
WT	0.11 ± 0.01	13.61 ± 0.06	0.0 ± 0.1
L-R90A	0.64 ± 0.04	12.54 ± 0.03	1.1 ± 0.1
L-R90Q	4.09 ± 1.03	11.49 ± 0.18	2.1 ± 0.2
H-G95A	26 ± 2	10.35 ± 0.05	3.3 ± 0.1
L-R90A, H-G95A	1400 ± 400	7.99 ± 0.17	5.6 ± 0.2
L-S91A, H-G95A	2400 ± 800	7.67 ± 0.20	5.9 ± 0.2

K_D was measured at equilibrium and 25 °C in solution by a competition ELISA. The $\Delta\Delta G$ values were calculated relative to the wild type. The mean and associated SE values of K_D, $\Delta G = -RT\ln(K_D)$, and $\Delta\Delta G = \Delta G(\text{wt}) - \Delta G(\text{mut})$ in at least three independent experiments are given. In addition, each ELISA measurement was done in triplicate. The SE value on $\Delta\Delta G$ was calculated through the formula $[SE(\Delta\Delta G)]^2 = [SE(\Delta G(\text{wt}))]^2 + [SE(\Delta G(\text{mut}))]^2$. wt, wild type; mut, mutant.

The L-CDR3 loop of the mutant Fab4E11(L-R90Q) had the following sequence: Gln90-Ser-Asn-Glu-Val-Pro-Trp-Thr97. This sequence is characteristic of the canonical structure 1 for the L-CDR3 loop of κ light chains (Al-Lazikani *et al*., 1997). The structure of the L-CDR3 loop of mAb4E11 (with L-Arg90) is close but clearly different from canonical structure 1, as found for example in the structure of Fab4-4-20, directed against fluorescein (Table 2) (Whitlow *et al*., 1995). An analysis of the torsion angles ϕ and ψ for residues L-90 to L-95 of scFv4E11 in its complex with ED3.DENV1 showed that they were close to those for canonical structure 1. In particular, L-Pro95 was in a *cis* conformation. However, the ψ angle of L-Trp96 and the ϕ angle of L-Thr97 differed widely from those of canonical structure 1, by 63.5 and 59.0 degrees, respectively (Table 3). This angle analysis was therefore consistent with mutation L-Q90R modifying the conformation of L-CDR3, its contacts with L-CDR1 and H-CDR3 and, indirectly, the interaction between Fab4E11 and ED3.

The L-CDR3 loop of mAb1A1D-2, directed against the ED3.DENV2 domain, has the following sequence: Gln90-Thr-Asn-Val-Asp-Pro-Trp-Ala97. This sequence is again characteristic of canonical structure 1. However, L-CDR3 is in a very different conformation in the crystal structure of the complex between Fab1A1D-2 and ED3.DENV2, with L-Pro95 in a *trans* conformation (Lok *et al*., 2008).

Long range effect of residue L-90

To experimentally demonstrate that mutations of residue L-90 have long range effects on the interaction between Fab4E11 and ED3.DENV1, we resorted to double-mutant thermodynamic cycles (Carter *et al*., 1984). Previously, we have reported that mutation H-G95A decreases the energy of interaction between Fab4E11 and ED3.DENV1 by 3.3 ± 0.1 kcal mol^{-1} (Bedouelle *et al*., 2006). The Cα atom of H-Gly95 is 29.5% accessible to the solvent in the complex between scFv4E11 and ED3.DENV1.

Table 2. Internal H-bonds of L-CDR3 in mAb4E11 and mAb4-4-20

mAb4E11 (3UZQ)	mAb4-4-20 (1FLR)
Cys88-O :: N-Gly99	Cys88-O :: N-Gly99
Gln89-Nε2 :: O-Trp96	Gln90-N :: O-Thr97
Arg90-N :: O-Thr97	Gln90-O :: N-Thr97
Arg90-Nη1 :: Oδ1-Asn92	Gln90-Oε1 :: N-Thr92
Arg90-Nε :: O-Pro95	Gln90-Oε1 :: N-His93
Arg90-Nη2 :: O-Pro95	Gln90-Oε1 :: Nδ1-His93
Pro95-O :: N-Thr97	Gln90-Nε2 :: O-His93
	Gln90-Nε2 :: O-Pro95[a]

The L-CDR3 sequence of mAb4-4-20 is 88CSQSTHVPWTFG99, whereas that of mAb4E11 is 88CQRSNEVPWTFG99.
[a]The distance between these two atoms (3.51 Å) is slightly too long for the formation of a H-bond. However, such an H-bond exists in the canonical structure 1 of L-CDR3 (Al-Lazikani *et al.*, 1997).

Table 3. Torsion angles of the residues in the L-CDR3 loops of mAb4E11 and canonical structure 1 (CS1)

Residue	Phi(4E11)	Psi(4E11)	Phi(CS1)	Psi(CS1)
90	−104.2	152.2	−96 ± 19	131 ± 16
91	−144.5	9.4	−122 ± 13	25 ± 12
92	−60.8	−40.4	−91 ± 23	−39 ± 12
93	−138.6	154.7	−128 ± 17	145 ± 22
94	−74.1	143.6	−86 ± 9	140 ± 9
95	−79.1	146.5	−74 ± 6	144 ± 7
96	−84.8	64.5	−66 ± 9	136 ± 8
97	−65.0	134.9	−130 ± 6	148 ± 9

The angles for the canonical structure 1 (CS1) of the κ light chains are given with their SD value (Al-Lazikani *et al.*, 1997). Residue 95 is a *cis*-Proline.

This Cα atom is in Van der Waals contact with water HOH501B, which, in turn, is strongly H-bonded with the main-chain O and side-chain Oε2 atoms of Glu309 in ED3.DENV1 (Figure 1C). Therefore, mutation H-G95A, which introduces an additional Cβ-H_3 group, likely creates a steric hindrance to the binding of Glu309.

We constructed two double mutants of Fab4E11, carrying mutations L-R90A and H-G95A for the first one, and L-S91A and H-G95A for the second one (Figure 1B). We chose these mutations for two reasons. First, the K_Ds of the double mutants had to be measurable, that is, not too large, even if the effects of the two mutations were additive. Second, we chose L-Ser91A as a control mutation because we expected that it would not perturb the conformation of L-CDR3 and that of H-CDR3 upstream of H-Trp96. Indeed, the Oγ-H group of L-Ser91 does not make any interaction with the remainder of L-CDR3 (Figure 1A) and it interacts with H-CDR3 only on the COOH side of H-Trp96 (Figure 1B). We measured the K_Ds of the double mutants exactly as performed for the single mutants of Fab4E11 (Table 1). The double mutant cycles showed that the effects of mutations L-S91A and H-G95A were strictly additive, that is, the effect of mutation H-G95A was the same in the context of the L-Ser91 residue as in that

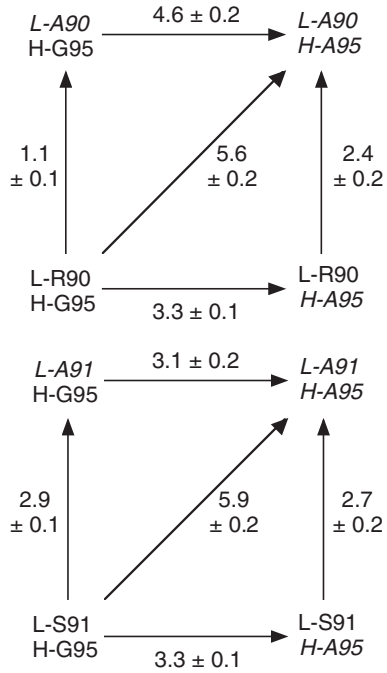

Figure 2. Thermodynamic cycles comparing the effects of single and double mutations in Fab4E11 on the free energy of interaction with ED3.DENV1. The mutant residues are indicated in italic type. The values of $\Delta\Delta G(H_2O)$ and associated SE (kcal mol^{-1}) at 25 °C were calculated from the values of $\Delta G(H_2O)$ and associated SE in Table 1 as described in Materials and Methods.

of L-Ala91. In contrast, the effects of mutations L-R90A and H-G95A were synergistic, that is, the effect of mutation H-G95A was 1.4 ± 0.2 kcal mol^{-1} higher in the context of L-Ala90 than in the context of L-Arg90 (Figure 2). Thus, the effect of mutation H-G95A on the interaction with the antigen depended on the residue side chain in position L-90. We concluded that the nature of the residue in position L-90, and in particular somatic hypermutation L-Q90R, affected the interaction between H-CDR3 and the antigen at a distance, through a conformational change.

Epitope transplantation

The K_D value for the interaction between Fab4E11 and its antigen is 50,000-fold larger for the ED3.DENV4 domain than for ED3.DENV1 (Cockburn *et al.*, 2012a). Four of the nine residues of ED3.DENV1 that are energetically important for its interaction with Fab4E11 are different in the DENV1 and DENV4 serotypes (Lisova *et al.*, 2007). To test whether these four differences of sequence were the cause of the difference in K_D, we progressively introduced the four residues that are present in ED3.DENV1 into ED3.DENV4. The single mutation S307K decreased 100-fold the value of K_D between ED3.DENV4 and Fab4E11 (Table 4). The simultaneous changes S307K, I308L, and D309E decreased 45,500-fold the value of K_D, down to that for ED3.DENV1. Finally, the four changes S307K, I308L, D309E, and M312V decreased K_D below that for ED3.DENV1, at the limit of our measuring abilities. These results confirmed the belonging of residues 307–312 to the energetic epitope of mAb4E11 and provided an explanation for the differences in affinity of Fab4E11 and neutralizing power of mAb4E11 between serotypes DENV1 and DENV4.

Table 4. Equilibrium constants and associated free energies for the dissociation between Fab4E11-H6 and variants of the ED3.DENV4-H6 domain

Variant	K_D (nM)	ΔG (kcal mol^{-1})	$\Delta\Delta G$ (kcal mol^{-1})
WT	4123 ± 745	7.36 ± 0.10	6.3 ± 0.1
S307K	13 ± 2	10.77 ± 0.09	2.9 ± 0.1
S307K-I308L-D309E	0.087 ± 0.027	13.81 ± 0.24	−0.2 ± 0.2
S307K-I308L-D309E-M312V	0.029 ± 0.009	14.37 ± 0.18	−0.7 ± 0.2

The $\Delta\Delta G$ values were calculated relative to ED3.DENV1-H6 ($K_D = 0.117 \pm 0.009$ nM; $\Delta G = 13.64 \pm 0.05$ kcal.mol^{-1}). K_D was measured at equilibrium and 25 °C in solution by a competition ELISA. The mean and associated SE values of K_D, ΔG, and $\Delta\Delta G$ in at least three independent experiments are given. In addition, each ELISA measurement was done in triplicate. See legend of Figure 1 for details.

Table 5. Equilibrium constants and associated free energies for the dissociation between Fab4E11-H6 and variants of the ED3.DENV1-H6 domain

Mutation	K_D (nM)	ΔG (kcal mol^{-1})	$\Delta\Delta G$ (kcal mol^{-1})
WT	0.117 ± 0.009	13.64 ± 0.05	0.0 ± 0.1
K307A	78 ± 10	9.71 ± 0.08	3.9 ± 0.1
K307V	19 ± 2	10.54 ± 0.05	3.1 ± 0.1
K307S	186 ± 59	9.25 ± 0.20	4.4 ± 0.2
L308A	4.1 ± 0.2	11.44 ± 0.02	2.2 ± 0.1
L308I	0.24 ± 0.05	13.15 ± 0.12	0.5 ± 0.1
E309A	0.7 ± 0.2	12.54 ± 0.14	1.1 ± 0.1
E309V	1.25 ± 0.04	12.14 ± 0.02	1.5 ± 0.1
E309K	103 ± 22	9.56 ± 0.12	4.1 ± 0.1
E309D	44 ± 5	10.04 ± 0.06	3.6 ± 0.1
V312A	1.3 ± 0.6	12.34 ± 0.20	1.3 ± 0.2
V312I	0.08 ± 0.04	13.96 ± 0.24	−0.3 ± 0.2
V312M	0.34 ± 0.07	12.95 ± 0.14	0.7 ± 0.1
L389A	2.1 ± 0.4	11.88 ± 0.15	1.8 ± 0.2
L389I	1.3 ± 0.4	12.27 ± 0.27	1.4 ± 0.3

The $\Delta\Delta G$ values were calculated relative to ED3.DENV1-H6. K_D was measured at equilibrium and 25 °C in solution by a competition ELISA. The mean and associated SE values of K_D, ΔG, and $\Delta\Delta G$ in at least three independent experiments are given. In addition, each ELISA measurement was done in triplicate. See legend of Figure 1 for details. The values for the mutations into Ala are from (Lisova *et al.*, 2007).

Non-conserved epitope residues within the DENV group

Many residues of ED3 that interact with scFv4E11 in the crystal structures are not conserved between DENV serotypes. Only 6 among the 23 residues of ED3 that make Van der Waals contacts with scFv4E11 and only 4 among the 16 residues that make intermolecular H-bonds are conserved between serotypes (Cockburn *et al.*, 2012a). The strictly conserved residues are Phe306, Lys310, Glu311, Asn366, Leu387, and Trp391 (DENV1 numbering). Phe306 makes contacts with scFv4E11 only through its main-chain O atom. Its side chain is fully buried in the protein core of ED3, it is strictly conserved in all flaviviruses and its change into Ala prevents the folding of ED3 (Lisova *et al.*, 2007). Lys310 is a major contributor to the energy of interaction between ED3.DENV1 and Fab4E11 with $\Delta\Delta G$(K310A) = 5.1 ± 0.2 kcal mol^{-1}. Glu311, Leu387, and Tyr391 are less important contributors with $\Delta\Delta G$ lower than 1.2 kcal mol^{-1} (Lisova *et al.*, 2007).

To analyze how the variations of residues between serotypes affect the interaction between Fab4E11 and ED3, we individually changed residues of ED3.DENV1 into those of the other serotypes. The results (Table 5) showed that Lys307 was a major contributor to the high affinity of Fab4E11 toward the DENV1 and DENV2 serotypes relative to DENV3 and DENV4 because both mutations K307V (toward DENV3) and K307S (toward DENV4) had the same effect as K307A, which totally deletes the side chain. Residue Glu309 is a moderate contributor to the interaction between Fab4E11 and ED3.DENV1 with $\Delta\Delta G$ (E309A) = 1.1 ± 0.1 kcal mol^{-1}. The contribution of its side chain was abolished by mutation E309V (toward DENV2) as by E309A. However, mutations E309K and E309D (toward DENV3 and DENV4) were highly detrimental to the interaction in the context of ED3.DENV1, with $\Delta\Delta G$(E309K) = 4.1 kcal mol^{-1} and $\Delta\Delta G$ (E309D) = 3.6 kcal mol^{-1}. The energetic consequences of a change into Ala are generally easier to interpret than other changes because it eliminates the side chain beyond the β carbon yet does not alter the main-chain conformation and does not impose electrostatic or steric effects (Cunningham and Wells, 1989; Reichmann *et al.*, 2007). However, we found puzzling that the variation of interaction energy toward Fab4E11 was larger between the wild-type ED3.DENV1 and its mutant ED3.DENV1 (E309K) ($\Delta\Delta G$ = 4.1 kcal mol^{-1}) than between ED3.DENV1 and ED3.DENV3 ($\Delta\Delta G = 2.7 \pm 0.1$ kcal mol^{-1}), even though ED3.DENV3 has Lys309 (see succeeding text) (Cockburn *et al.*, 2012a).

Structural context of the epitope residues and antigenicity

To understand why some mutations had a higher detrimental effect on the interaction between Fab4E11 and ED3.DENV1 than the simple deletion of the side chain by mutation into Ala, we modeled the mutations in the structure of the complex between scFv4E11 and ED3.DENV1, using the What If program, and we recorded the resulting clashes between residues, that is, Van der Waals contacts at distances lower than 3.20 Å. This analysis showed that the mutant residue Lys309 would make steric clashes directly with residue H-Arg94 of scFv4E11, which makes numerous interactions with Lys325 and Glu362 (Figure 1C). The mutant residue Asp309 would make steric clashes with Lys325 and Pro364 in ED3.DENV1 and would thus affect the interactions of Lys325 with H-Arg94 and H-Tyr102 in H-CDR3 and of Pro364 with H-Asp31 in H-CDR1 (not shown). Likewise, the effect of the rather conservative mutation L308I could be explained by a mild steric clash directly with H-Trp96 (Figure 1C), and those of V312M and L389I by steric clashes with neighboring residues in ED3.DENV1. We controlled that these clashes did not exist in the structures of the complexes between scFv4E11 and the DENV serotypes that natively carry the mutated residues. Thus, the mutations in ED3.DENV1 that deleted part of a residue side chain were easier to interpret than those that added groups of

atoms. Some of the latter had an effect on the energy of interaction between Fab4E11 and ED3.DENV1 that was more important that the deletion of the side chain by mutation into Ala. These results indicated that the function of a residue in folding or binding depended on its structural environment and thus on serotype.

Hydrophobic pocket in ED3

We have previously shown that the triad of aliphatic residues Leu/Ile308, Val/Ile/Met312, and Leu/Ile389 in the ED3 domains of the four DENV serotypes, which participates in the formation of a hydrophobic pocket at the surface of the dengue virion, is replaced by bulky residues, Trp/Phe, Pro, and His/Tyr, respectively, in all the other *Flaviviruses*. We proposed that these bulky residues could be the cause for the lack of binding between Fab4E11 and *Flaviviruses* that do not belong to the dengue group, and therefore, that the epitope of mAb4E11 constitutes an antigenic signature of the DENV group of *Flaviviruses* (Lisova *et al*., 2007). Moreover, a superimposition of the ED3 domain from tick-borne encephalitis virus (TBEV; protein data bank [PDB] accession 1SVB) onto that from DENV1 in complex with scFv4E11 (PDB 3UZQ) showed a clash between residues His390 of ED3.TBEV (His389 with DENV1 numbering) and residue L-Tyr28 of scFv4E11, which would prohibit Fab4E11 binding (Cockburn *et al*., 2012a).

To test these assumptions experimentally, we changed the three corresponding residues of ED3.DENV1 into residues that are present in *Flaviviruses* outside of the DENV group, that is, Leu308 into Phe, Val312 into Pro, and Leu389 into Tyr or His. The mutant ED3.DENV1 domains were correctly folded because their λ_{max} of fluorescence emission was within 1.0 nm of that for the parental ED3.DENV1 (342.5 nm), and they had no detectable free Cys residue in an Ellman's test, that is, their disulfide bond was formed. The L308F, L389Y, and L389H mutations abolished the interaction between Fab4E11 and ED3.DENV1 to undetectable levels. In contrast, the K_D for the interaction between Fab4E11 and the mutant ED3.DENV1(V312P) was equal to 0.307 ± 0.072 nM and thus very close to the value for the parental ED3.DENV1 domain, 0.117 ± 0.009 nM. Thus, our mutational analysis confirmed the essential role of the aliphatic pocket at the surface of ED3 for the recognition between the DENV viruses and mAb4E11, but did not explain why Pro312 is conserved in all *Flaviviruses* except those of the DENV group.

DISCUSSION

Typology of the interfacial water molecules

Statistical analysis of protein–protein complexes and of their interfaces has led to the classification of the interfacial water molecules in three sets, according to the energy of their interactions: (i) water molecules making favorable interactions with both proteins; (ii) those making favorable interactions with only one protein; and (iii) those making no interaction with either protein (Ahmed *et al*., 2011). We used the WHAT IF program, which calculates the energy of H-bonds on a scale extending from 0 to 1, to identify the indirect interactions, mediated by water molecules, between scFv4E11 and the ED3 domains of the four DENV serotypes and to classify them. Most interfacial water molecules between scFv4E11 and ED3 made H-bonds with both protein partners: 10 out of 12 for DENV1, 6/7 for DENV2 and DENV3, and 9/12 for DENV4. A small proportion of interfacial water molecules made H-bonds with one partner and Van der Waals interactions with the other partner. Finally, two water molecules, HOH455A and HOH56B, made only Van der Waals interactions with both scFv4E11 and ED3.DENV4 (Supplementary Table S1). The proportion of interfacial water molecules making H-bonds with both protein partners was approximately equal for all four serotypes, 82% on average, and much higher that the proportion of 21% in protein–protein complexes of similar crystallographic resolutions (Rodier *et al*., 2005; Ahmed *et al*., 2011).

The location of HOH56B is not specific to the interface between svFv4E11 and ED3.DENV4. Indeed, water molecules, HOH507B and HOH74A respectively, are present at the same location in the interface between scFv4E11 and either ED3.DENV1 or ED3.DENV2, where they make H-bonds with both protein partners (Supplementary Table S1). HOH455A could be superficially classified as having no favorable interaction with either protein, scFv4E11 or ED3.DENV4. However, it makes a strong H-bond with HOH105B, which, in turn, is firmly H-bonded to both Lys310(Nζ) and Lys323(Nζ) of ED3.DENV4 (Supplementary Table S2). Analyzing the doubly indirect interactions may help refine the classification of water molecules at interfaces.

The conservation of interfacial water molecules and of their interactions between DENV serotypes (Results) suggests that they play a role in the interaction or recognition between scFv4E11 and the ED3 domain. The high proportion of interfacial water molecules making H-bonds with both scFv4E11 and ED3 suggests that they could facilitate the cross-recognitions between scFv4E11 and the four serotypes of ED3.

Comparison between interfaces of high and low affinities

The affinity of scFv4E11 is 50,000-fold higher for ED3.DENV1 than for ED3.DENV4 (Cockburn *et al*., 2012a). We therefore compared the interfaces of the two complexes in detail (Supplementary Table S3). Previously, the interfacial residues between protein partners have been divided in three classes, according to the interaction type: (i) dry spots make direct H-bonds with the other partner; (ii) wet spots make H-bonds with the other partner only through a water molecule; and (iii) dual spots make both direct and water mediated H-bonds (Teyra and Pisabarro, 2007). We found that 4 residues of ED3.DENV1 could be ranked as dry, 3 as wet, and 6 as dual. Similarly, 6 residues of ED3.DENV4 could be ranked as dry, 2 as wet, and 6 as dual. We also ranked each acceptor or donor group of H-bonds in the same way. We found that 10 groups of ED3.DENV1 could be ranked as dry, 8 as wet, and 3 as dual. Similarly, 11 groups of ED3.DENV4 could be classified as dry, 6 as wet, and 3 as dual. As expected on the basis of their acceptor or donor abilities, the groups that we classified as dual spots were the main-chain O atom, the lysine Nζ-H_3 group, the aspartate Oδ atoms, the glutamate Oε atoms and, on the scFv4E11 side, the arginine Nη-H_2 and tyrosine Oη-H groups. The proportion of wet residues, 23% for ED3.DENV1 and 14% for ED3.DENV4 were consistent with those reported in a statistical analysis (Teyra and Pisabarro, 2007). The classification by donor/acceptor group rather than by residue showed a higher proportion of wet interactions, provided a more accurate description of the interfaces and underlined the importance of water in the recognition between scFv4E11 and ED3. This analysis did not show substantial differences between ED3.DENV1 and ED3.DENV4 in the number of elements (amino acid residues or atomic groups) in each class.

More generally, we compared the numbers of direct and indirect interactions between scFv4E11 and either ED3.DENV1 or ED3.DENV4 and obtained the following figures: direct H-bonds, 15 versus 17; indirect interactions through one water molecule, 12 versus 12; indirect interactions through two water molecules, 5 versus 10 (Supplementary Tables S1 to S3). In addition, each of ED3.DENV1 and ED3.DENV4 make direct Van der Waals interactions with 37 residues of scFv4E11 (Cockburn *et al*., 2012a). Therefore, there are similar numbers of direct and singly indirect H-bonds between scFv4E11 and its antigens, as reported in statistical analyses of other protein–protein complexes (Rodier *et al*., 2005; Teyra and Pisabarro, 2007). We did not find differences in the interfacial water molecules or their interactions between a complex of high affinity (i.e. with ED3.DENV1) and a complex of low affinity (i.e. with ED3.DENV4) other than a higher number of doubly indirect interactions, mediated by two water molecules, for ED3.DENV4. More detailed physicochemical parameters are needed to explain the wide difference of affinity between these two antigens, for example, their electrostatic fields as previously described (Cockburn *et al*., 2012a). In this respect, some of the water molecules involved in doubly-indirect interactions may counterbalance the excess of negative charges at the surface of ED3.DENV4 relative to the other DENV serotypes.

Indirect interactions mediated by complementarity determining regions

We found that mutations in the L-CDR3 loop of mAb4E11, which does not form any contact with its antigen, strongly and indirectly affected its affinity for the antigen. In particular, we found that somatic hypermutation L-Q90R increased the affinity for the antigen indirectly, without forming a direct bond or contact with it, by modifying the conformation of L-CDR3 and hence, its interactions with the neighboring CDRs. Numerous experiments of *in vitro* directed evolution, aimed at improving the affinity of recombinant antibodies, have shown that the beneficial mutations often do not contact the antigen directly (Foote and Winter, 1992; Lavoie *et al*., 1992; Hawkins *et al*., 1993; Schildbach *et al*., 1993; Wedemayer *et al*., 1997). Here, we provided detailed structural mechanisms for such indirect interactions. We also provided experimental evidence, through double mutant thermodynamic cycles.

Energetic hotspot residues of the epitope and their structural context

The exchange of residues between serotypes of the antigen showed that the contribution of an ED3 residue to the energy of interaction with Fab4E11 depended on its structural context and therefore serotype. This conclusion is illustrated by the two following results. (i) We changed residue Lys307 into Ser307 in both contexts of ED3.DENV1 and ED3.DENV4. The variation of interaction energy $\Delta\Delta G$ toward Fab4E11 was equal to 4.39 ± 0.21 kcal mol^{-1} between ED3.DENV1 and its mutant ED3.DENV1(K307S) (Table 5) and to 3.41 ± 0.13 kcal mol^{-1} between the mutant ED3.DENV4 (S307K) and ED3.DENV4 (Table 4), that is, a difference of 0.98 ± 0.25 kcal mol^{-1}. (ii) We transplanted the epitope of Fab4E11 from ED3.DENV1 into ED3.DENV4 through four changes of residues and found that three of them, at positions 307, 308, and 309, were sufficient to increase 45,500-fold the affinity of Fab4E11 for ED3.DENV4, up to the level of that for ED3.DENV1. However, the fourth change, at position 312, increased the affinity above that for ED3.DENV1 (Table 4). Therefore, the variations of antigenicity according to the ED3 serotype cannot be apprehended only through variations of sequences. The structural environment of a residue is important. We also found that two residues in a hydrophobic pocket at the surface of ED3 were responsible for the specificity of mAb4E11 for the *Flaviviruses* of the DENV group.

CONCLUSION

Our study provided insights into the role of water in the recognition between mAb4E11 and the four serotypes of its DENV antigen. It also described and documented a precise mechanism for the indirect role of a somatic hypermutation in the increase of affinity between antibody and antigen through CDRs conformational changes. Finally, it stressed that sequence comparisons alone cannot explain the cross-reactivities of an antibody toward different serotypes (or strains) of its antigen and that bound water molecules and the structural context of the epitope are important. Our results should contribute to improve our understanding of the indirect interactions between antibodies and viral antigens and, more generally, between proteins. They could be useful to engineer these interactions, through antibody engineering, antigen engineering or the design of inhibitors, in particular to obtain therapeutic molecules or improved vaccines against the dengue virus.

REFERENCES

Ahmed MH, Spyrakis F, Cozzini P, Tripathi PK, Mozzarelli A, Scarsdale JN, Safo MA, Kellogg GE. 2011. Bound water at protein-protein interfaces: partners, roles and hydrophobic bubbles as a conserved motif. *PLoS One* **6**: e24712.

Al-Lazikani B, Lesk AM, Chothia C. 1997. Standard conformations for the canonical structures of immunoglobulins. *J. Mol. Biol.* **273**: 927–948.

de Alwis R, Beltramello M, Messer WB, Sukupolvi-Petty S, Wahala WM, Kraus A, Olivarez NP, Pham Q, Brien JD, Tsai WY, Wang WK, Halstead S, Kliks S, Diamond MS, Baric R, Lanzavecchia A, Sallusto F, de Silva AM. 2011. In-depth analysis of the antibody response of individuals exposed to primary dengue virus infection. *PLoS Negl. Trop. Dis.* **5**: e1188.

Austin SK, Dowd KA, Shrestha B, Nelson CA, Edeling MA, Johnson S, Pierson TC, Diamond MS, Fremont DH. 2012. Structural Basis of Differential Neutralization of DENV-1 Genotypes by an Antibody that Recognizes a Cryptic Epitope. *PLoS Pathog.* **8**: e1002930.

Babu JP, Pattnaik P, Gupta N, Shrivastava A, Khan M, Rao PV. 2008. Immunogenicity of a recombinant envelope domain III protein of dengue virus type-4 with various adjuvants in mice. *Vaccine* **26**: 4655–4663.

Barillari C, Taylor J, Viner R, Essex JW. 2007. Classification of water molecules in protein binding sites. *J. Am. Chem. Soc.* **129**: 2577–2587.

Batra G, Nemani SK, Tyagi P, Swaminathan S, Khanna N. 2011. Evaluation of envelope domain III-based single chimeric tetravalent antigen and monovalent antigen mixtures for the detection of anti-dengue antibodies in human sera. *BMC Infect. Dis.* **11**: 64.

Bedouelle H, Belkadi L, England P, Guijarro JI, Lisova O, Urvoas A, Delepierre M, Thullier P. 2006. Diversity and junction residues as hotspots of binding energy in an antibody neutralizing the dengue virus. *FEBS J.* **273**: 34–46.

Beltramello M, Williams KL, Simmons CP, Macagno A, Simonelli L, Quyen NT, Sukupolvi-Petty S, Navarro-Sanchez E, Young PR, de Silva AM, Rey FA, Varani L, Whitehead SS, Diamond MS, Harris E, Lanzavecchia A, Sallusto F. 2010. The human immune response to Dengue virus is dominated by highly cross-reactive antibodies endowed with neutralizing and enhancing activity. *Cell Host Microbe* **8**: 271–283.

Brandler S, Lucas-Hourani M, Moris A, Frenkiel MP, Combredet C, Fevrier M, Bedouelle H, Schwartz O, Despres P, Tangy F. 2007. Pediatric measles vaccine expressing a dengue antigen induces durable

serotype-specific neutralizing antibodies to dengue virus. *PLoS Negl. Trop. Dis.* **1**: e96.
Brandler S, Ruffie C, Najburg V, Frenkiel MP, Bedouelle H, Despres P, Tangy F. 2010. Pediatric measles vaccine expressing a dengue tetravalent antigen elicits neutralizing antibodies against all four dengue viruses. *Vaccine* **28**: 6730–6739.
Carter PJ, Winter G, Wilkinson AJ, Fersht AR. 1984. The Use of Double Mutants to Detect Structural-Changes in the Active-Site of the Tyrosyl-Transfer Rna-Synthetase (Bacillus-Stearothermophilus). *Cell* **38**: 835–840.
Chen R, Vasilakis N. 2011. Dengue--quo tu et quo vadis? *Viruses* **3**: 1562–1608.
Chen Y, Maguire T, Marks RM. 1996. Demonstration of binding of dengue virus envelope protein to target cells. *J. Virol.* **70**: 8765–8772.
Chen S, Yu M, Jiang T, Deng Y, Qin C, Qin E. 2007. Induction of tetravalent protective immunity against four dengue serotypes by the tandem domain III of the envelope protein. *DNA Cell Biol.* **26**: 361–367.
Chen HW, Liu SJ, Li YS, Liu HH, Tsai JP, Chiang CY, Chen MY, Hwang CS, Huang CC, Hu HM, Chung HH, Wu SH, Chong P, Leng CH, Pan CH. 2013. A consensus envelope protein domain III can induce neutralizing antibody responses against serotype 2 of dengue virus in non-human primates. *Arch. Virol.* **158**: 1523–1531.
Chin JF, Chu JJ, Ng ML. 2007. The envelope glycoprotein domain III of dengue virus serotypes 1 and 2 inhibit virus entry. *Microbes Infect.* **9**: 1–6.
Cockburn JJ, Navarro Sanchez ME, Fretes N, Urvoas A, Staropoli I, Kikuti CM, Coffey LL, Arenzana Seisdedos F, Bedouelle H, Rey FA. 2012a. Mechanism of dengue virus broad cross-neutralization by a monoclonal antibody. *Structure* **20**: 303–314.
Cockburn JJ, Navarro Sanchez ME, Goncalvez AP, Zaitseva E, Stura EA, Kikuti CM, Duquerroy S, Dussart P, Chernomordik LV, Lai CJ, Rey FA. 2012b. Structural insights into the neutralization mechanism of a higher primate antibody against dengue virus. *EMBO J.* **31**: 767–779.
Cunningham BC, Wells JA. 1989. High-resolution epitope mapping of hGH-receptor interactions by alanine-scanning mutagenesis. *Science* **244**: 1081–1085.
Elahi M, Islam MM, Noguchi K, Yohda M, Kuroda Y. 2013. High resolution crystal structure of dengue-3 envelope protein domain III suggests possible molecular mechanisms for serospecific antibody recognition. *Proteins* **81**: 1090–1095.
Etemad B, Batra G, Raut R, Dahiya S, Khanam S, Swaminathan S, Khanna N. 2008. An envelope domain III-based chimeric antigen produced in Pichia pastoris elicits neutralizing antibodies against all four dengue virus serotypes. *Am. J. Trop. Med. Hyg.* **79**: 353–363.
Foote J, Winter G. 1992. Antibody framework residues affecting the conformation of the hypervariable loops. *J. Mol. Biol.* **224**: 487–499.
Gromowski GD, Barrett ND, Barrett AD. 2008. Characterization of dengue virus complex-specific neutralizing epitopes on envelope protein domain III of dengue 2 virus. *J. Virol.* **82**: 8828–8837.
Guzman MG, Hermida L, Bernardo L, Ramirez R, Guillen G. 2010. Domain III of the envelope protein as a dengue vaccine target. *Expert Rev. Vaccines* **9**: 137–147.
Halstead SB, Mahalingam S, Marovich MA, Ubol S, Mosser DM. 2010. Intrinsic antibody-dependent enhancement of microbial infection in macrophages: disease regulation by immune complexes. *Lancet Infect. Dis.* **10**: 712–722.
Hawkins RE, Russell SJ, Baier M, Winter G. 1993. The contribution of contact and non-contact residues of antibody in the affinity of binding to antigen. The interaction of mutant D1.3 antibodies with lysozyme. *J. Mol. Biol.* **234**: 958–964.
Holbrook MR, Shope RE, Barrett AD. 2004. Use of recombinant E protein domain III-based enzyme-linked immunosorbent assays for differentiation of tick-borne encephalitis serocomplex flaviviruses from mosquito-borne flaviviruses. *J. Clin. Microbiol.* **42**: 4101–4110.
Huang KC, Lee MC, Wu CW, Huang KJ, Lei HY, Cheng JW. 2008. Solution structure and neutralizing antibody binding studies of domain III of the dengue-2 virus envelope protein. *Proteins* **70**: 1116–1119.
Huerta V, Chinea G, Fleitas N, Sarria M, Sanchez J, Toledo P, Padron G. 2008. Characterization of the interaction of domain III of the envelope protein of dengue virus with putative receptors from CHO cells. *Virus Res.* **137**: 225–234.
Hung JJ, Hsieh MT, Young MJ, Kao CL, King CC, Chang W. 2004. An external loop region of domain III of dengue virus type 2 envelope protein is involved in serotype-specific binding to mosquito but not mammalian cells. *J. Virol.* **78**: 378–388.
Jaiswal S, Khanna N, Swaminathan S. 2004. High-level expression and one-step purification of recombinant dengue virus type 2 envelope domain III protein in Escherichia coli. *Protein Expr. Purif.* **33**: 80–91.
Janin J. 1999. Wet and dry interfaces: the role of solvent in protein-protein and protein-DNA recognition. *Structure with Folding & Design* **7**: R277–R279.
Khanam S, Pilankatta R, Khanna N, Swaminathan S. 2009. An adenovirus type 5 (AdV5) vector encoding an envelope domain III-based tetravalent antigen elicits immune responses against all four dengue viruses in the presence of prior AdV5 immunity. *Vaccine* **27**: 6011–6021.
Lavoie TB, Drohan WN, Smith-Gill SJ. 1992. Experimental analysis by site-directed mutagenesis of somatic mutation effects on affinity and fine specificity in antibodies specific for lysozyme. *J. Immunol.* **148**: 503–513.
Lisova O, Hardy F, Petit V, Bedouelle H. 2007. Mapping to completeness and transplantation of a group-specific, discontinuous, neutralizing epitope in the envelope protein of dengue virus. *J. Gen. Virol.* **88**: 2387–2397.
Lok SM, Ng ML, Aaskov J. 2001. Amino acid and phenotypic changes in dengue 2 virus associated with escape from neutralisation by IgM antibody. *J. Med. Virol.* **65**: 315–323.
Lok SM, Kostyuchenko V, Nybakken GE, Holdaway HA, Battisti AJ, Sukupolvi-Petty S, Sedlak D, Fremont DH, Chipman PR, Roehrig JT, Diamond MS, Kuhn RJ, Rossmann MG. 2008. Binding of a neutralizing antibody to dengue virus alters the arrangement of surface glycoproteins. *Nat. Struct. Mol. Biol.* **15**: 312–317.
Matsui K, Gromowski GD, Li L, Schuh AJ, Lee JC, Barrett AD. 2009. Characterization of dengue complex-reactive epitopes on dengue 3 virus envelope protein domain III. *Virology* **384**: 16–20.
Midgley CM, Bajwa-Joseph M, Vasanawathana S, Limpitikul W, Wills B, Flanagan A, Waiyaiya E, Tran HB, Cowper AE, Chotiyarnwong P, Grimes JM, Yoksan S, Malasit P, Simmons CP, Mongkolsapaya J, Screaton GR. 2011. An in-depth analysis of original antigenic sin in dengue virus infection. *J. Virol.* **85**: 410–421.
Midgley CM, Flanagan A, Tran HB, Dejnirattisai W, Chawansuntati K, Jumnainsong A, Wongwiwat W, Duangchinda T, Mongkolsapaya J, Grimes JM, Screaton GR. 2012. Structural analysis of a dengue cross-reactive antibody complexed with envelope domain III reveals the molecular basis of cross-reactivity. *J. Immunol.* **188**: 4971–4979.
Modis Y, Ogata S, Clements D, Harrison SC. 2003. A ligand-binding pocket in the dengue virus envelope glycoprotein. *Proc. Natl. Acad. Sci. U. S. A.* **100**: 6986–6991.
Modis Y, Ogata S, Clements D, Harrison SC. 2005. Variable surface epitopes in the crystal structure of dengue virus type 3 envelope glycoprotein. *J. Virol.* **79**: 1223–1231.
Pattnaik P, Babu JP, Verma SK, Tak V, Rao PV. 2007. Bacterially expressed and refolded envelope protein (domain III) of dengue virus type-4 binds heparan sulfate. *J. Chromatogr. B Analyt. Technol. Biomed. Life Sci.* **846**: 184–194.
Pryor MJ, Carr JM, Hocking H, Davidson AD, Li P, Wright PJ. 2001. Replication of dengue virus type 2 in human monocyte-derived macrophages: comparisons of isolates and recombinant viruses with substitutions at amino acid 390 in the envelope glycoprotein. *Am. J. Trop. Med. Hyg.* **65**: 427–434.
Reichmann D, Cohen M, Abramovich R, Dym O, Lim D, Strynadka NC, Schreiber G. 2007. Binding hot spots in the TEM1-BLIP interface in light of its modular architecture. *J. Mol. Biol.* **365**: 663–679.
Rodier F, Bahadur RP, Chakrabarti P, Janin J. 2005. Hydration of protein-protein interfaces. *Proteins* **60**: 36–45.
Roehrig JT, Butrapet S, Liss NM, Bennett SL, Luy BE, Childers T, Boroughs KL, Stovall JL, Calvert AE, Blair CD, Huang CY. 2013. Mutation of the dengue virus type 2 envelope protein heparan sulfate binding sites or the domain III lateral ridge blocks replication in Vero cells prior to membrane fusion. *Virology* **441**: 114–125.
Sabin AB. 1952. Research on dengue during World War II. *Am. J. Trop. Med. Hyg.* **1**: 30–50.
Sangkawibha N, Rojanasuphot S, Ahandrik S, Viriyapongse S, Jatanasen S, Salitul V, Phanthumachinda B, Halstead SB. 1984. Risk factors in dengue shock syndrome: a prospective epidemiologic study in Rayong, Thailand. I. The 1980 outbreak. *Am. J. Epidemiol.* **120**: 653–669.
Schildbach JF, Near RI, Bruccoleri RE, Haber E, Jeffrey PD, Novotny J, Sheriff S, Margolies MN. 1993. Modulation of Antibody-Affinity by a Noncontact Residue. *Protein Sci.* **2**: 206–214.

Schmitz J, Roehrig J, Barrett A, Hombach J. 2011. Next generation dengue vaccines: a review of candidates in preclinical development. *Vaccine* **29**: 7276–7284.

Simmons M, Nelson WM, Wu SJ, Hayes CG. 1998a. Evaluation of the protective efficacy of a recombinant dengue envelope B domain fusion protein against dengue 2 virus infection in mice. *Am. J. Trop. Med. Hyg.* **58**: 655–662.

Simmons M, Porter KR, Escamilla J, Graham R, Watts DM, Eckels KH, Hayes CG. 1998b. Evaluation of recombinant dengue viral envelope B domain protein antigens for the detection of dengue complex-specific antibodies. *Am. J. Trop. Med. Hyg.* **58**: 144–151.

Simmons CP, Farrar JJ, van Vinh Chau N, Wills B. 2012. Dengue. *N. Engl. J. Med.* **366**: 1423–1432.

Simonelli L, Beltramello M, Yudina Z, Macagno A, Calzolai L, Varani L. 2010. Rapid structural characterization of human antibody-antigen complexes through experimentally validated computational docking. *J. Mol. Biol.* **396**: 1491–1507.

Simonelli L, Pedotti M, Beltramello M, Livoti E, Calzolai L, Sallusto F, Lanzavecchia A, Varani L. 2013. Rational engineering of a human anti-dengue antibody through experimentally validated computational docking. *PLoS One* **8**: e55561.

Smith SA, de Alwis R, Kose N, Durbin AP, Whitehead SS, de Silva AM, Crowe JE, Jr. 2013. Human monoclonal antibodies derived from memory B cells following live attenuated dengue virus vaccination or natural infection exhibit similar characteristics. *J. Infect. Dis.* **207**: 1898–1908.

Teyra J, Pisabarro MT. 2007. Characterization of interfacial solvent in protein complexes and contribution of wet spots to the interface description. *Protein Struct. Funct. Bioinformatics* **67**: 1087–1095.

Thullier P, Demangel C, Bedouelle H, Megret F, Jouan A, Deubel V, Mazie JC, Lafaye P. 2001. Mapping of a dengue virus neutralizing epitope critical for the infectivity of all serotypes: insight into the neutralization mechanism. *J. Gen. Virol.* **82**: 1885–1892.

Volk DE, Lee YC, Li X, Thiviyanathan V, Gromowski GD, Li L, Lamb AR, Beasley DW, Barrett AD, Gorenstein DG. 2007. Solution structure of the envelope protein domain III of dengue-4 virus. *Virology* **364**: 147–154.

Vriend G. 1990. WHAT IF: a molecular modeling and drug design program. *J. Mol. Graph.* **8**: 52–56.

Watterson D, Kobe B, Young PR. 2012. Residues in domain III of the dengue virus envelope glycoprotein involved in cell-surface glycosaminoglycan binding. *J. Gen. Virol.* **93**: 72–82.

Wedemayer GJ, Patten PA, Wang LH, Schultz PG, Stevens RC. 1997. Structural insights into the evolution of an antibody combining site. *Science* **276**: 1665–1669.

Whitlow M, Howard AJ, Wood JF, Voss EW, Jr., Hardman KD. 1995. 1.85 A structure of anti-fluorescein 4-4-20 Fab. *Protein Eng.*. **8**: 749–761.

Zhang Y, Zhang W, Ogata S, Clements D, Strauss JH, Baker TS, Kuhn RJ, Rossmann MG. 2004. Conformational changes of the flavivirus E glycoprotein. *Structure* **12**: 1607–1618.

Zhang ZS, Yan YS, Weng YW, Huang HL, Li SQ, He S, Zhang JM. 2007. High-level expression of recombinant dengue virus type 2 envelope domain III protein and induction of neutralizing antibodies in BALB/C mice. *J. Virol. Methods* **143**: 125–131.

Zhang X, Sheng J, Plevka P, Kuhn RJ, Diamond MS, Rossmann MG. 2013a. Dengue structure differs at the temperatures of its human and mosquito hosts. *Proc. Natl. Acad. Sci. U. S. A.* **110**: 6795–6799.

Zhang X, Ge P, Yu X, Brannan JM, Bi G, Zhang Q, Schein S, Zhou ZH. 2013b. Cryo-EM structure of the mature dengue virus at 3.5-A resolution. *Nat. Struct. Mol. Biol.* **20**: 105–110.

Zidane N, Dussart P, Bremand L, Villani ME, Bedouelle H. 2013a. Thermodynamic stability of domain III from the envelope protein of flaviviruses and its improvement by molecular design. *Protein Eng. Des. Sel.* **26**: 389–399.

Zidane N, Ould-Abeih MB, Petit-Topin I, Bedouelle H. 2013b. The folded and disordered domains of human Ribosomal Protein SA have both idiosyncratic and shared functions as membrane receptors. *Biosci. Rep.* **33**: 113–124. doi:10.1042/BSR20120103.

Zidane N, Dussart P, Bremand L, Bedouelle H. 2013c. Cross-reactivities between human IgMs and the four serotypes of dengue virus as probed with artificial homodimers of domain-III from the envelope proteins. *BMC Infect. Dis.* **13**: 302.

SUPPORTING INFORMATION

Additional supporting information may be found in the online version of this article at the publisher's web site.